Chapter 22

Scattering from Magnetically Oriented Microtubule Biopolymers

Wim Bras[1], Gregory P. Diakun[2], Richard C. Denny[2], Anthony Gleeson[2], Claudio Ferrero[3], Yehudi K. Levine[4], and J. Fernando Díaz[5]

[1]Netherlands Organisation for Scientific Research (NWO), DUBBLE CRG/ESRF, BP 220 F38043 Grenoble Cedex, France
[2]CCLRC Daresbury Laboratory, Warrington WA4 4AD, United Kingdom
[3]European Synchrotron Radiation Facility, BP 220 F38043 Grenoble Cedex, France
[4]Utrecht University, Debye Institute, Section for Computational Biophysics, P.O. Box 80000, 3508 TA Utrecht, Netherlands
[5]KU Leuven, Laboratory for Chemical and Biological Dynamics, Celestijnenlaan, 200 D, Leuven, Belgium

Microtubules are biopolymers with a large number of functions in all eukaryotic cells. The study of their physical behaviour is complex due to their dynamic self-assembly and disassembly. Attempts to orient the hydrated, and therefore biological viable form, by conventional methods like shearing are hampered by their fragility and their extreme length which allows them only to be oriented in small domains inside a larger disoriented surrounding. For experiments like X-ray fibre diffraction this is not satisfactory. We have developed a method to align these long molecules by assembling them in a controlled way inside a strong magnetic field (7-10 Tesla). This method can possibly be applied to other molecules which resist other methods of alignment but which have sufficient sources of diamagnetism built into their structure. Sources of diamagnetism are for instance regular arrays of peptide bonds (like α-helices and β-sheets), aromatic rings or double and triple C-bonds. Successful fibre diffraction experiments to 18 Å resolution have been obtained with this method. The rather gentle forces applied to the magnetic field and the slow disorientation makes this method extremely suitable for experiments where one wants to study the interaction between molecules and reduce the number of degrees of orientational freedom. This method can also be applied to other bio- or synthetic polymers in solution.

© 2000 American Chemical Society

Introduction

Microtubules play several important roles in the cell. They are involved in intra-cellular transport, motility, mitosis and form an important part of the cytoskeleton [1]. They consist of long chains of tubulin protein dimers, called protofilaments, which connect laterally to form a hollow cylindrical structure with an external diameter of approximately 30 nm and a length which can extend to micrometers. The number of protofilaments can vary between 11 and 17 but the pre-dominant number in a normal functioning cell is 13. The persistence length of these polymers is reported to be between 2000 - 5200 μm [2,3] so that for most experiments they can be considered to be a rigid rod system. The length distribution is influenced by the biochemical conditions and fluctuates due to dynamic assembly/disassembly properties. With the biochemical conditions in these experiments the average length is approximately 5 μm [4] giving an average molecular weight of 10^9 Dalton. Amino acid sequencing shows that the homology in the tubulin protein between organisms as wildly varying as yeast to pigs and humans is at least 75% [5]. The structure of the basic building block, the tubulin dimer, has recently been solved [6] but the structure of the assembled molecule is still not known in detail. Structural properties are important parameters for the study of the (self)assembly mechanism and the interactions with other ligands like for instance anti-cancer drugs.

We have reported previously on Small Angle X-ray Scattering experiments (SAXS) aimed at the elucidation of the structure. The preparation of hydrated, and therefore biologically interesting, samples suitable for small angle X-ray fibre diffraction is not trivial. The only reasonable successful method has been centrifugation over extended lengths of time (>24 hours) and subsequent rehydration [7]. With this method one is not guaranteed that the brute force approach has not changed the structure nor that the rehydration is complete. With other methods like Couette and flow shearing it is possible to create small oriented domains in an otherwise isotropic sample. These domains, however, do not retain their orientation very long and even small temperature gradients are sufficient to distort the system [8,9]. An additional problem is that the molecules only scatter weakly so that, even using a synchrotron radiation source, many hours of data collection are needed in order to obtain a satisfactory statistical data quality.

Diamagnetism can be found in many molecules. The principle sources are aromatic groups, double and triple C-bonds and peptide bonds. In α-helices and β-sheets all the amino acids are in a single plane and can be added vectorially thus creating a possible source of relatively strong diamagnetism. We have investigated the possibility to orient microtubules making use of the interaction between their small diamagnetic moments and high magnetic field. For some polymers this interaction is sufficient to create fully aligned samples, notably for rigid polymers with a low molecular weight containing aromatic groups which are rigidly bound to the backbone. However, this is exception and in general this method is not usable due to a combination of too low a diamagnetic moment and steric hindering which prevents the alignment. For self assembling (bio)polymers like actin and fibrinogen it has been shown that the assembly inside the magnetic field will result in the production of nearly fully aligned samples [10, 11]. This method can also be applied to synthetic polymers in which case it becomes possible to study the aligned samples in solution

but which can also be thought of as a possible method to create highly aligned solid samples by first assembling the molecules and subsequently evaporating the solvent. With the relatively low prices for modern strong superconducting magnets this method, pioneered several decades ago, might nowadays be a feasible method for creating highly aligned speciality polymers, like for instance electroluminescent ones, which are difficult to align in solution, on an industrial scale.

On theoretical grounds and using the average molecular weight value and assuming that the main contribution to the diamagnetic moment is due to α-helices with an orientation parallel to the tubulin dimer axis, which make up roughly 25% of the total amount of amount of amino acids [6], and thus to the microtubule axis, the diamagnetic moment of the microtubule can be calculated to be approximately to be $\Delta\chi_{//} \approx 1.01 \times 10^{-28}\, m^3$ for which it can be calculated that a minimum magnetic field strength of ≈ 6 T is required to obtain some degree of alignment [12]. Experimentally it has been found that in fields of approximately 11 T the maximum degree of alignment is obtained [12].

From real time magnetic birefringence experiments it was found that the reaction rate is an important parameter for the achievement of full alignment [12]. In these experiments the sample is placed in a strong magnetic field and the birefringence, Δn, is measured either as function of the variable magnetic field strength or as function of other sample parameters, like for instance temperature, whilst the magnetic field is kept constant. For low concentration samples, in a limited orientation range, the measured birefringence has a linear relation with the degree of orientation of the molecules. Contrary to intuition, which predicts that the best alignment will be obtained when the reaction rates are slow so that the molecules have time to align in the field we have found that fast reactions are the best method, see figure 1. This can be understood when one looks at the number of nucleation sites for elongation in the solution. When this number is high, which is generally the case for fast reactions, the overall polymer length will be relatively short. However, these polymers can be sufficiently large to overcome the potential barrier for alignment and be the aligned 'seeds' from which further polymerisation can take place. With less nucleation sites and thus longer molecules the elongated polymers will be locked in their orientation due to steric hindering effects. For polymers with a long persistence length it is even possible that the field can be switched off and that they still retain this orientation even in solutions or in some cases that the orientation even increases with time. This has been previously observed with other self assembling macromolecules [10, 13]. This property has enabled us to perform fibre diffraction studies on these molecules by aligning them off-line and then transporting them to a Synchrotron Radiation beamline, see figure 2.

For rigid rod molecules with an axial ration of 50 - 200 without any constraint applied to them, Flory predicted that the angular distribution of the long axis would be at most 10.2° - 11° [14, 15]. In the case of microtubules this prediction has been confirmed by experiments in which it was shown that the maximum obtainable degree of alignment of microtubules aligned in a high magnetic field but then taken out of the field so that the constraint was removed, was roughly 10° [12]. The analysis of the fibre diffraction pattern is therefore rather difficult since the degree of alignment is such that at higher q-values the reflections belonging to the layer lines can start to overlap with the diffraction arcs from the equator or other layer lines. For the low resolution data this proved to be not too much of a problem. In figure 3 the

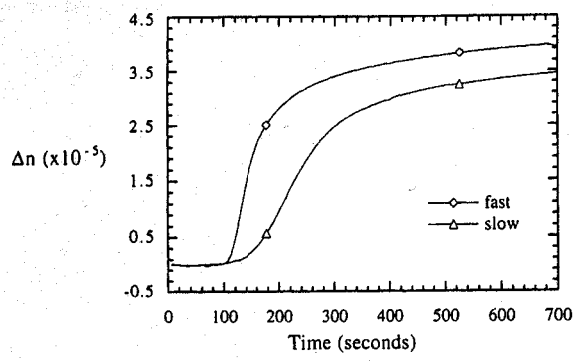

Figure 1
Magnetic birefringence experiments on microtubules assembled inside a 12 T magnetic field. The birefringence, Δn, is a measure of the degree of alignment. Initially the polymers are unassembled and give no birefringence. Once the assembly starts the signal increases. Fast assembly rates give the highest birefringence and orientation. Figure taken from [13].

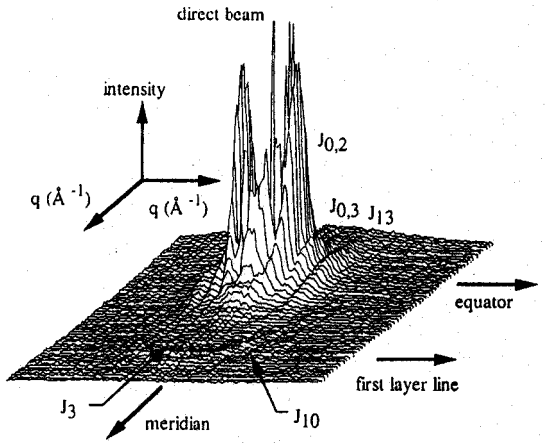

Figure 2
Three dimensional representation of a low angle X-ray fibre diffraction pattern of magnetically oriented microtubules in which the X-ray beam was at right angles with the polymer long axis. The pattern can be analysed in helical diffraction terms. The orders of the Bessel functions assigned to each peak are indicated. The peaks indicated with $J_{0,n}$ are due to the cylindrical structure, the peak indicated by J_{13} is predominantly due the modulations of the outside cylinder wall. Total data collection time was longer than 2 hours.

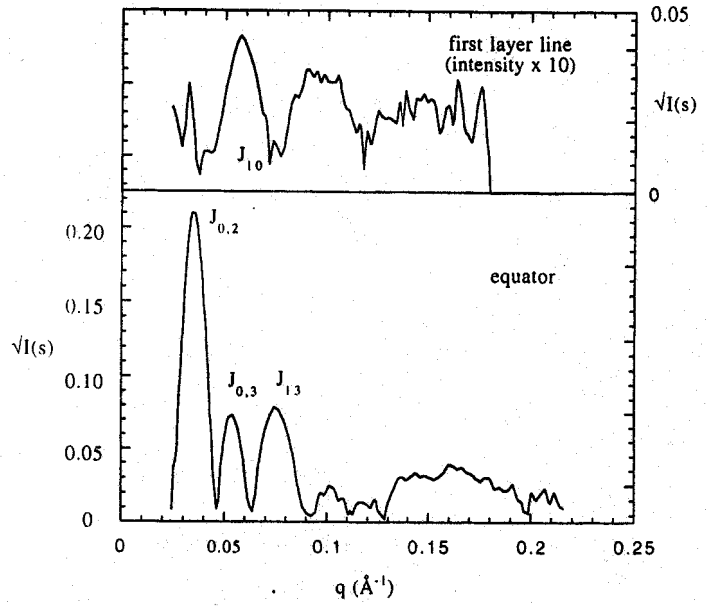

Figure 3
Equatorial and first layer line intensities of the microtubule fibre diffraction pattern shown in figure 2. The vertical intensity axis is in arbitrary intensity units. The layer line intensity is very weak compared to the equatorial intensity which makes the mathematical correction for the spread in the angular orientation very difficult. For this reason an alternative method of data collection and interpretation is use as described in the text.

diffracted intensity on the equator and the first layer line is shown. To obtain these curves it was necessary to correct for the disorientation and several geometrical parameters. For this the CCP13 suite of software was used [12, 16, 17]. Due to the longitudinal staggering of the different protofilaments the surface of microtubules have shallow helical grooves running over them so that the diffraction pattern has to be explained in terms of helical diffraction theory [18, 19].

Algorithms, used for the mathematical correction of the disorientation effects on the diffraction peaks in general requires a high signal to noise ratio in order to render reliable results. In order to increase the accuracy of the determination of the real diffraction intensities and to avoid software induced systematic errors for the higher order diffraction peaks, where the signal to noise ratio is low, a different method has been tried. In this case the microtubules were aligned with their axis parallel to the X-ray beam. This means that one only observes the scattering pattern from the equatorial plane and thus avoid the overlap between the different reflections. An additional advantage is that it is also possible in this case to perform a radial integration over the full area of the two dimensional detector, thus increasing the statistics considerably. This allows one to study the low angle range where the interparticle scattering contributes considerably to the scattering intensity. Biologically this is interesting since the interdistance between microtubules in part determines their function in the cell.

Materials and Methods

The protein tubulin was purified from pig brains and prepared for experiments as described elsewhere [20]. The protein concentration was determined spectrophotometrically. For assembly the tubulin was equilibrated with 10 mM sodium phosphate, 3.4 M glycerol, 1 mM EDTA, 0.1 mM GTP buffer (pH 7.0) after which 1 mM GTP and the desired concentration of $MgCl_2$ were added. The sample were centrifuged for 10 minutes at 50,000 rpm at 4° C to eliminate aggregates. Assembly could be initiated by raising the temperature from 4° C to 37° C. The samples were assembled and aligned in a 9 T magnetic field before being transported to the SAXS beamline.

For these experiments the Small Angle X-ray Scattering beamline 2.1 of the SRS at the CLRC Daresbury laboratory was used. This beamline has been described in detail [20] and only a short description is given. For these experiments a gas filled proportional counter with an active area of 200 x 200 mm^2 was used. This photon counting device has been shown to be the most useful detector for this type of work since the low intrinsic background and the absence of read-out noise allow the proper subtraction of the scattering background due to the buffer solution, air scatter and contributions from the cell windows. The electron density difference of the microtubules with respect to the buffer solution is rather small and therefore the proper subtraction is of crucial importance especially in the high q-range. The sample to detector distance was chosen to be 2 and 9 meters covering a scattering vector range from $2 \times 10^{-2} < q < 1.8 \times 10^{-1}$ Å^{-1} and $4 \times 10^{-3} < q < 5 \times 10^{-2}$ Å^{-1} respectively, where the former experiment was performed to see what the effect of interparticle scattering was.

Radiation damage was prevented by using elongated cells which were slowly translated through the beam. Optical inspection showed that the damaged areas remain localised and that no transport of material through the cell took place on the time scales of the experiments.

Results

As mentioned in the introduction the accurate determination of the scattered intensity in a sample with a low degree of alignment is a non-trivial exercise especially when this intensity is small with respect to the intrinsic background, due to the buffer solution and unassembled material. For equatorial data there is the possibility to determine these intensities from samples aligned with their long axis parallel to the X-ray beam so that we only probe the equatorial plane which is a projection of the molecule on its basal plane. This will now be a circular symmetric pattern. See Figure 4.

Figure 5 shows the low angle scattering pattern from three different concentrations of microtubules in glycerol assembly buffer. The long microtubule axis was coincident with the X-ray beam so that we are only observing the intensity from the equatorial plane of the molecule. The insert shows the very low angle data, where the effects of interparticle scattering are visible. For this concentration range the (theoretical) interdistance has been calculated to be varying from 1800 - 2600 Å. It was calculated that the system is in the dilute regime.

In the very low q-region, where effects due to interparticle scatter will be most pronounced, we indeed find a concentration dependent effect in as such that the scattered intensity, corrected for the different protein concentration, is stronger for the lower concentrations. To gain a better insight some simulations were performed.

The interference effects arising from the packing of the microtubules in a sample were estimated by considering the sample to be a two-dimensional disordered fluid. The microtubules were represented as hard, hollow discs with an inner radius of 86 Å outer radius of 146 Å. These discs were placed at random in a square box of side 10 000 Å. The average distance between the centres of the discs was varied by changing the number of discs in the box. The packing of N discs into the box was carried out under the constraint that the distance r_{nm} between the centres of any two discs n and m in the box was $r_{nm} \geq 286$Å, in order to avoid unphysical overlap. The initial configuration of the discs in the box was changed by allowing each disc to undergo a random displacement with maximum amplitude of 16 Å. The disc to be moved was chosen at random and its displacement was accepted provided it did not overlap any other discs in the box. A new configuration was produced after attempting a displacement of every disc in the box. The simulation proceeded by generating up to 16 000 configurations and evaluating the diffracted intensity I_L using the positions of the centres of the discs for every fifth configuration. I_L was calculated using the expression $I_L(\vec{q}) = I_D(\vec{q}) \sum_{n,m} exp[-i\vec{q}.\vec{r}]$ where I_D is the scattered intensity from single hollow discs and q is the wave vector. In practice, only $I_L(q_x)$ was calculated, as the scattered intensity was found to be symmetric in the $\{q_x, q_y\}$ plane as expected. The average distance between the centres of the discs in the box was calculated simultaneously. We evaluated the scattered intensities from configurations containing

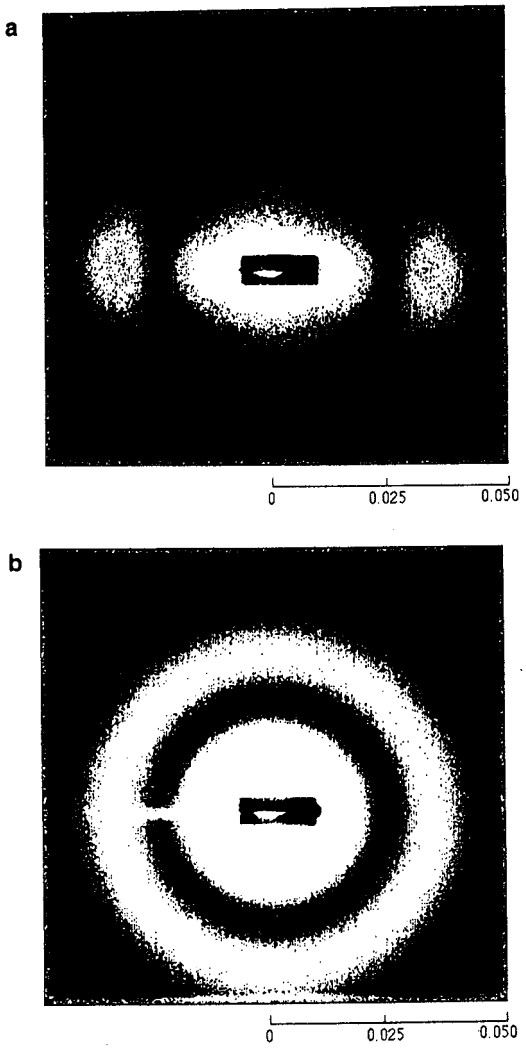

Figure 4
Small angle scattering patterns from microtubules aligned with the long axis at right angles to the X-ray beam (panel a) and with the long axis parallel with the X-ray beam (panel b). The scale is in $q=2\pi/d$ ($Å^{-1}$).

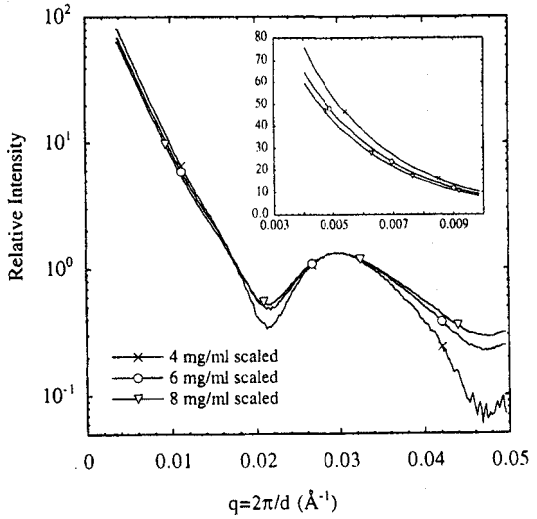

Figure 5
The low angle scattering pattern from microtubules aligned with their long axis parallel to the incident beam for 3 different concentrations. The insert is a magnification of the lowest q-range (with a linear abscissa) showing the effects of interparticle scattering. This effect is much stronger than found in simulated data. This possibly can be due to a non-random distribution of polymers in the samples through clustering in bundles. This will give rise to a locally higher concentration.

between 50 and 700 discs, covering an average nearest centre-to-centre distances between 1000 Å and 330 Å. The computational time ranged from 30 minutes at the dilute end to 24 hours for a system of 700 discs. The number of configurations used was chosen judiciously so as to yield statistical fluctuations of less than 3% in the diffracted intensity. The differences in the simulated intensities between different concentration are approximately a factor of 5 less than the experimental values shown in the insert of figure 5, although the tendency for higher central scatter with lower protein concentration remains. This can indicate that the average distance distribution is deviating from that of a complete random distribution and that actually bundles of microtubule polymers are formed. In such a scenario the interparticle scatter will be dominated by the distance distribution inside such a bundle apparently giving a much stronger concentration effect.

The radius of gyration of the cross section, R_C, can be calculated from the Guinier approximation [21].

$$I(q) = I(0)e^{-\frac{q^2R_c^2}{2}}$$

For cylindrical scattering objects the R_C is related to the dimensions of the cylinder according to:

$$R_c^2 = \frac{R_{outer}^2 + R_{inner}^2}{2} + \frac{h^2}{12}$$

Experimentally it was determined that this value ranged between 167 - 160 Å. Since the length, h, is not in the observed scattering range so it can be assumed that this length will not contribute to the scattering and only the first term remains. If we now take the dimer dimension in the radial direction, i.e. the cylinder wall thickness, to be 65 Å [1] and thus substituting $R_{inner} = R_{outer} - 65$ Å, we can calculate that the external radius is between 170 - 180 Å. This is larger than expected on the basis of electron microscopy and earlier scattering results. These results can be influenced by the large degree of length polydispersity. However, these values have been used as the starting parameters in the fitting procedure described below.

Helical diffraction theory [18] tells us that the scattering pattern on the equator of the fibre diffraction pattern can be explained as a combination of a Fourier transform of the basic hollow cylinder modulated by cylindrical Bessel functions of the order corresponding with the symmetry in the basal plane. This can be approached in two equivalent ways. The first one uses a J_0 Bessel function to describe the cylinder and the convolutes this with an unknown function H(q) which represents the shape of the cylinder wall. Another approach is to use the Fourier transform (FT) of a basic hollow cylinder and then add the Bessel function describing these modulations on the bases of intelligent guesses. This has clear analytical advantages. The FT of a smooth walled hollow cylinder is given by [22]:

$$F(q) = R_{outer}\frac{J_1(qR_{outer})}{q} - R_{inner}\frac{J_1(qR_{inner})}{q}$$

The walls of this cylinder will be modulated by electron density grooves between neighbouring protofilaments, both on the inner and outer wall. Due to the 13 fold symmetry this can be expressed as J_{13} Bessel functions with arguments $J_{13}(qR_{inner}+\Delta_{inner})$ and $J_{13}(qR_{outer}-\Delta_{outer})$. The magnitude of the Δ_{inner} and Δ_{outer} reflects the depth of the grooves on the cylinder wall. From a preliminary

analysis it can be seen that the contribution due to the modulation of the inner wall falls outside the scattering range observed in this study but that the modulation due to the outer wall can add scattered intensity in the observed scattering range at $q > 0.1$ Å^{-1}. An initial fit to the experimental data with an expression based on equation (1) was therefore limited to the range $q < 0.1$ Å^{-1} where is certain that no other contributions will be present. As a starting parameter for the fitting procedure the values obtained via the calculations based on the R_C were used. This resulted in a best fit to the data of a cylinder with an $R_{outer} = 146\pm5$ Å and an $R_{inner} = 86\pm5$ Å, see figure 6. The subsequent addition and fit of a contribution of a J_{13} Bessel function relating to the outside wall over a data range that covers the region $q > 0.1$ Å^{-1} shows that the grooves between the protofilaments are roughly 21 Å deep. The subsequent addition of contributions of the grooves on the inside wall has not been performed yet since at this moment no reliable data obtained from samples aligned with their axis parallel to the X-ray beam is available yet for that data range. Once this data is available the next step will be to reconstruct the equatorial intensity trace and compare this with solution scattering and fibre diffraction patterns in order to be able to deconvolute the overlap between the higher q-range of the equator and the layer lines.

The first layer line can be found on a line with a meridional q-value of ≈ 0.157 Å^{-1}. As mentioned in the introduction the degree of alignment is not extremely high and this means that in the equatorial q-range above 0.157 Å^{-1} it is possible that reflections will start to overlap. However, by using the method of first determining the accurate intensities at lower q on the equator and then fitting these with the appropriate analytical functions it is possible to deconvolute the intensities coming from layer lines. In fact it might be better, once the equatorial diffraction pattern is accurately determined, to revert back to scattering from randomly oriented samples for the deconvolution procedure. This method is being investigated at the moment.

Conclusions

Although not extensively discussed in this work magnetic birefringence has shown that magnetic fields only have to be applied for a limited time during the onset of polymerisation in order to create aligned samples in solution. On the basis of these results it can be predicted that this method of sample preparation might be applied to suitable synthetic polymers as well. This can provide a way to study the molecular transform without interference due to inter-molecular interactions. With a fast reaction the sample only has to remain in the field for several seconds and thus provides the possibility to develop this method into a polymer processing technique.

The application of helical diffraction theory in combination with experiments on suitably oriented molecules allows us to introduce a step wise fitting procedure with which we first can use knowledge of the basic cylindrical structure of the molecule, then add the Bessel function terms relating to the modulations on the cylindrical surface. The next step is to compare these data with solution scattering patterns in order to be able to deconvolute the equatorial and layer line intensities. Once this model is completed the positions of the dimers in the microtubule wall will be known and the scattering parameters obtained from the known dimer structure can

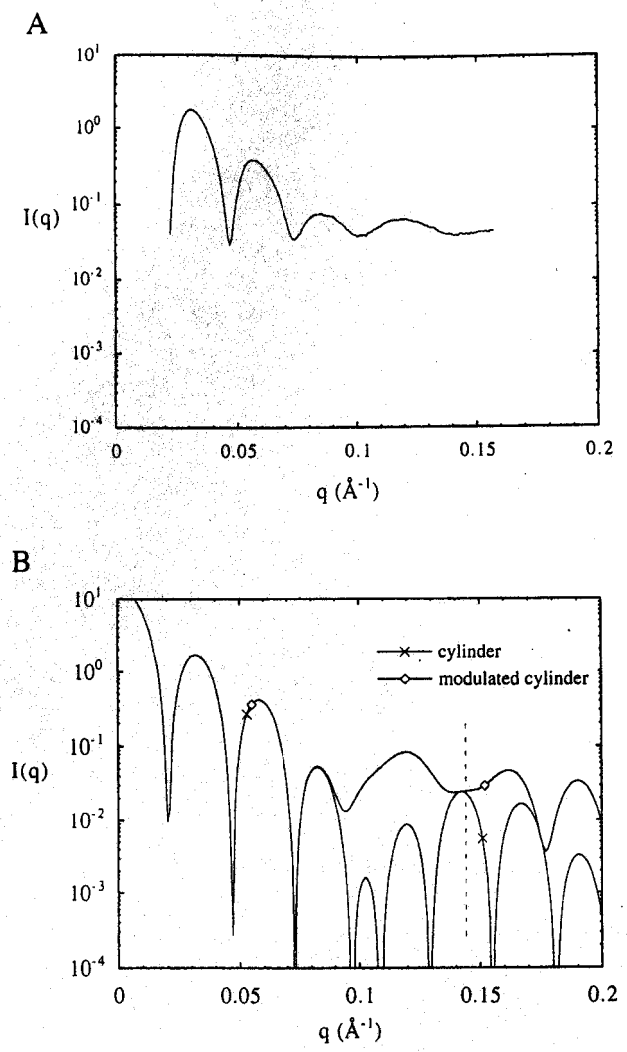

Figure 6
Scattered intensity from microtubules aligned with their long axis parallel to the X-ray beam (panel a). This is equivalent to the equatorial data obtained from a fibre diffraction pattern but one is certain that neither systematic errors due to mathematical procedures used for correction of the angular spread of the molecules are seen nor intensity due to overlap from diffraction arcs of the layer lines. Panel b shows the best fits (χ^2 = 0.05) to the data using the fitting procedure described in the text. The dotted line indicates the maximum extend of the experimental data at present. The line indicated with 'cylinder' is the contribution of two J_1 functions describing the basic cylinder. The 'modulated' curve is the real fit taking into account the modulations on the cylinder surface.

be used to refine the model with respect to fibre diffraction data. The last step to describe the system is to calculate the interaction between microtubules in solution. Modelling studies describing the interparticle interference effects are being carried out at the moment and indeed show qualitative agreement with the experimental data but give a strong indication that the microtubules are not randomly positioned in the samples but are forming larger bundles.

Hansgerd Kramer and Georg Maret are gratefully acknowledged for their help in the birefringence experiments. Liz Towns-Andrews and Sue Slawson of CCLRC Daresbury Laboratory have been very helpful with the fibre diffraction experiments. Eric v.d. Zee has assisted in some of the diffraction experiments.

Literature Cited

1. *Structure of microtubules* ed. K.Roberts and J.S Hyams Academic Press 1979
2. F.Gittes, B.Mickey, J.Nettleton, J.Howard *J.of Cell Biol.*, 1993, 120(4), 923-934
3. P.Venier, A.C.Maggs, M.F.Carlier, D.Pantaloni *J.Biol.Chem.*, 1994, 269(18), 13353-13360
4. F.Pirollet, D.Job, R.Margolis, J.Garel *EMBO journal* 6(11), 1987, 3247-3252
5. P.Valanzuela, M. Quiroga, J.Zaldivar, W.J.Rutter, M.W. Kirschner, D.W.Cleveland *Nature* 289,1981, 650-655
6. E.Nogales, S. Grayer-Wolf, I.A.Khan, R.F.Luduena, K.H.Downing *Nature* 375, 1995, 424-427
7. E. Mandelkow *Methods in Enzymology* 134, 1986, 149-168
8. J.Nordh, J.Deinum, B.Norden *Eur.Biophys.J.*, 14, 1986, 113-122
9. R.E.Buxbaum, T.Dennerl, S.Weiss, S.R.Heidemann *Science* 235, 1987, 1511-1514
10. J.Torbet, M. Ronzière *Biochem.J.*219(1984) 1057-1059
11. J.Torbet *Biochemistry* 25, 1986, 5309-5314
12. W.Bras, G.P. Diakun, J.F.Díaz, G. Maret , H.Kramer, J.Bordas, F.J. Medrano *Biophysical Journal* 74(3), 1998, 1509
13. W. Bras *PhD thesis Liverpool John Moores University* 1995
14. A.Suzuki, T.Maeda, T.Ito *Biophys. J.*, 1991, 59, 25-30)
15. P.J. Flory *Proc. Royal. Soc. London* A234, 1956, 73-89
16. http://www.dl.ac.uk/SRS/CCP13/main.html
17. R.C. Denny *Private communication*
18. A.Klug, F.Crick, H.Wyckoff *Acta.Cryst.*, 11, 1958, 199-213
19. L.A. Amos , A.Klug, 1974, *J.Cell.Sci.* 14, 523-549
20. J.M. Andreu, J.Bordas, J.F. Díaz, J. Garcia de Ancos, R.Gil, F.J.Medrano, E,Nogales, E.Pamtos, E.Towns-Andrews *J.Mol. Biol.* 226,1992, 169-184
21. Towns-Andrews E., A.Berry, J.Bordas, G.R.Mant, P.K.Murray, K.Roberts, I.S.Sumner, J.S.Worgan, R.Lewis. *Rev.Sci.Instr.*60(7), 1989, 2346 - 2349
22. O. Glatter in *Small Angle X-ray scattering* ed. O.Glatter, O.Kratky Academic Press 1982
23. *Diffraction of X-rays by chain molecules* B.K. Vainshtein Elsevier 1966

About the Cover

The art was provided by N. S. Murthy, W. Tang, and K. Zero of AlliedSignal Inc. from a fully drawn fiber of a copolymer of PET obtained at the Advanced Polymers Beamline X27C in the National Synchrotron Light Source, Brookhaven National Laboratory.

ACS SYMPOSIUM SERIES 739

Scattering from Polymers

Characterization by X-rays, Neutrons, and Light

Peggy Cebe, EDITOR
Tufts University

Benjamin S. Hsiao, EDITOR
University of New York at Stony Brook

David J. Lohse, EDITOR
Exxon Research and Engineering Company

American Chemical Society, Washington, DC

Library of Congress Cataloging-in-Publication Data

Scattering from polymers : characterization by x-rays, neutrons, and light / Peggy Cebe, editor, Benjamin S. Hsiao, editor, David J. Lohse, editor.

p. cm.—(ACS symposium series, ISSN 0097-6156 ; 739)

Developed from a symposium sponsored by the Division of Polymeric Materials: Science and Engineering, at the 216th National Meeting of the American Chemical Society, Boston, Mass., August 21–27, 1998.

Includes bibliographical references and index.

ISBN 0-8412-3644-5

1. Polymers—Analysis Congresses. 2. Scattering (Physics)—Congresses.

I. Cebe, Peggy. II. Hsiao, Benjamin S. III. Lohse, David J. IV. American Chemical Society. Division of Polymeric Materials: Science and Engineering. V. American Chemical Society. Meeting (216th : 1998 : Boston, Mass.) VI. Series.

QD139.P6S4 1999
547'.7046—dc21 99-35339
CIP

The paper used in this publication meets the minimum requirements of American National Standard for Information Sciences—Permanence of Paper for Printed Library Materials, ANSI Z39.48–1984.

Copyright © 2000 American Chemical Society

Distributed by Oxford University Press

All Rights Reserved. Reprographic copying beyond that permitted by Sections 107 or 108 of the U.S. Copyright Act is allowed for internal use only, provided that a per-chapter fee of $20.00 plus $0.50 per page is paid to the Copyright Clearance Center, Inc., 222 Rosewood Drive, Danvers, MA 01923, USA. Republication or reproduction for sale of pages in this book is permitted only under license from ACS. Direct these and other permission requests to ACS Copyright Office, Publications Division, 1155 16th St., N.W., Washington, DC 20036.

The citation of trade names and/or names of manufacturers in this publication is not to be construed as an endorsement or as approval by ACS of the commercial products or services referenced herein; nor should the mere reference herein to any drawing, specification, chemical process, or other data be regarded as a license or as a conveyance of any right or permission to the holder, reader, or any other person or corporation, to manufacture, reproduce, use, or sell any patented invention or copyrighted work that may in any way be related thereto. Registered names, trademarks, etc., used in this publication, even without specific indication thereof, are not to be considered unprotected by law.

PRINTED IN THE UNITED STATES OF AMERICA

Advisory Board

ACS Symposium Series

Mary E. Castellion
ChemEdit Company

Arthur B. Ellis
University of Wisconsin at Madison

Jeffrey S. Gaffney
Argonne National Laboratory

Gunda I. Georg
University of Kansas

Lawrence P. Klemann
Nabisco Foods Group

Richard N. Loeppky
University of Missouri

Cynthia A. Maryanoff
R. W. Johnson Pharmaceutical Research Institute

Roger A. Minear
University of Illinois at Urbana–Champaign

Omkaram Nalamasu
AT&T Bell Laboratories

Kinam Park
Purdue University

Katherine R. Porter
Duke University

Douglas A. Smith
The DAS Group, Inc.

Martin R. Tant
Eastman Chemical Co.

Michael D. Taylor
Parke-Davis Pharmaceutical Research

Leroy B. Townsend
University of Michigan

William C. Walker
DuPont Company